The October 2023 annular eclipse: some effects on HF propagation

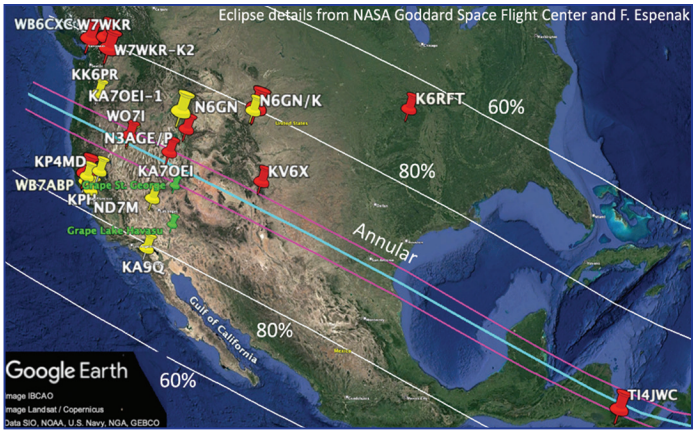

FIGURE 1: Path of the 14 October 2023 annular eclipse showing locations of FST4W transmitters (red) and receivers (yellow) within the zone at least 60% obscured. Credit Google Earth and eclipse data from NASA Goddard Space Flight Center and F. Espenak.

There have been remarkable advances in affordable amateur-radio equipment, digital-communications protocols, open-access databases and analysis methods, since the 2015 partial eclipse over the UK.

Drawing on those advances, this article describes some impacts of reduced absorption and lowered F2 critical frequency (foF2) on HF propagation during the 14 October 2023 eclipse over North America.

Introduction

These methods and results contributed to the Festival of Eclipse Ionospheric Science, an initiative of the Ham Radio Citizen Science Investigation (HamSCI) [1]. **Figure 1** shows the path of the annular eclipse, tracking southeast from Oregon to Costa Rica. In an annular eclipse, the Moon does not entirely cover the Sun, but it leaves visible a 'ring of fire'. Within the 60 per cent obscured zone, map pins show stations that used FST4W, a beacon-like digital mode within the WSJT-X package [2]. The receivers logged signal-to-noise ratio (SNR), as with WSPR and FT8, and also noise level [3] and frequency spread [4], [5] using the WsprDaemon package [6]. These transmitters and receivers used low-cost GPS-aided or GPS-disciplined oscillators, reducing frequency jitter to less than a few tens of milliHertz. Given this level of stability, eclipse-induced changes to propagation modes could be identified.

Reduced D region absorption

Steve, G0KYA, in his *RadCom* article on the 2015 eclipse, introduced the science of how an eclipse affects propagation from VLF upward [7]. On a normal morning, as UV radiation from the rising Sun ionises the ionosphere's D region, absorption increases on the lower HF bands. As a result, sky-wave signal levels drop. If the receiving site has low local noise, noise propagated in from distant sources will be absorbed. The SNR, measured by FST4W and other digital modes, reflects changes in both signal and noise levels. To see the transient effects of the eclipse on absorption properly, we need to separate SNR out to independent signal and noise levels.

Noise level and SNR

My example is from the 560km path on 3.5MHz between Tom, WO7I (Nevada, DN10cw), and KFS, a historic maritime radio station (Half Moon Bay, 33km SSE of San Francisco, California, CM87tj). The transmitter at WO7I was a novel WsprSonde with 1W output simultaneously on six HF bands [8]. At KFS, the receiver was a multi-band KiwiSDR. **Figure 2** shows the noise level and SNR prior to and during the eclipse. Instead of reducing smoothly, following the cosine of the solar zenith angle (the angle between the Sun's elevation and the zenith), the noise level showed a plateau and a lift. The eclipse reduced UV radiation to the D region, allowed ions and electrons to recombine, thereby reducing absorption. This led to a higher-than-usual noise level for the time of day. The SNR of the WO7I signal also rose during the eclipse for the same reason. Note the asymmetry in rise between the eclipse start and maximum, and between the maximum and the end. This is a feature seen on other paths and by other methods, and merits further investigation.

Signal level

The SNR's usefulness as a proxy for signal level is compromised whenever noise level varies. However, simple addition of the SNR and noise level scaled to 2.5kHz bandwidth yields the signal level (**Figure 3**). The model line is the product of the cosine of the solar zenith angle, to represent the daily pattern, and one minus the eclipse obscuration function (EOF). The EOF, a time series of the percentage of the Sun's area obscured by the Moon at the mid-point of the path, was computed using the Astropy package [9].

In Figure 3, there is a close match in shape and timing of the peak between the signal level and the model. This brings to life what handbooks tell us: recombination of electrons and ions in the D region, leading to reduced absorption, is fast – seconds to minutes [10].

Lowered foF2

The eclipse also facilitates ion-electron recombination in the F2 layer, leading to a transient reduction in the F2 critical frequency (foF2). I'll describe two examples where FST4W frequency spread could identify changes in propagation modes.

Mixed two-hop and one-hop becomes one-hop

With an effective sunspot number (SSNe) of 125 for the days spanning the eclipse, PyLap ray-tracing [11] showed a mix of two-hop and one-hop propagation on 14MHz for the 1808km path between Dick, W7WKR (Washington State, CN97uj), and Dan, KV6X (New Mexico, DM75aq), **Figure 4**. The two-hop path was via the F2 layer at 36° ray elevation, and a one-hop E region path at 3°, a low elevation. This mixed-mode propagation prediction was consistent with the frequency spread generally exceeding 100mHz on days other than the 14th, and on the 14th other than after the eclipse maximum (at 1637UTC), **Table 1**. That eclipse-affected interval, outlined in blue in Table 1, had a frequency spread less than 50mHz, consistent with one-hop propagation.

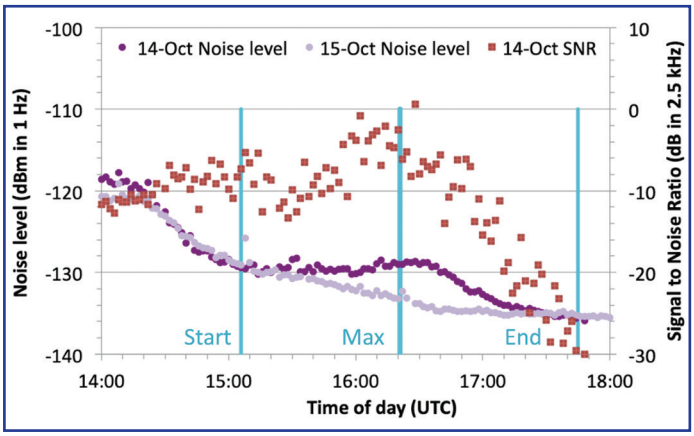

FIGURE 2: Time series of noise level at 3.5MHz at KFS on 14 and 15 October 2023, showing the higher level of propagated-in noise because of reduced absorption during the eclipse. Superimposed are the eclipse-day SNR of FST4W transmissions from WO7I.

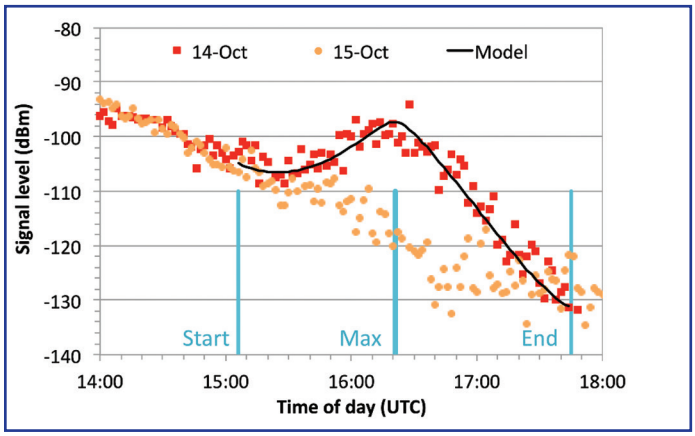

FIGURE 3: Time series of signal level for WO7I at KFS on 3.5MHz on 14 October 2023, derived from SNR and noise level. Superimposed (black) is a scaled level from a simple model.

Knowing that the propagation was via one-hop during the second half of the eclipse, the SSNe in PyLap could be reduced, by trial and error, until two-hop rays landed further than 1808km from the transmitter. This happened at an SSNe value of 70. The annular eclipse with 84 per cent of the Sun's surface obscured was equivalent to the SSN dropping temporarily from 125 to 70.

The transition from mixed-mode to one-hop took place around, and after, the eclipse maximum, showing that the ionospheric response was delayed. This was in contrast with the immediate effect of reduced absorption on signal level, shown in Figure 3. There are two related reasons for the delay: first, recombination of ions and electrons in the F2 layer is much slower than in the D region [10], and second, the critical frequency had to drop low enough to push all two-hop ray landing spots to over 1808km range.

One-hop transition to the two-ray zone, and side scatter

Having seen mixed two- and one-hop propagation temporarily transition to one hop, what happened on a marginal one-hop path as foF2 fell? Results on the 1056km path between W7WKR and KPH (Point Reyes, 58km NW of San Francisco, California, CM88mc) on 14MHz led to interesting answers. A scatter plot of frequency spread against signal level for 14 October between 1442UTC and 2000UTC is shown in **Figure 5**, where we can discern three regions:

1. A tight cluster with high signal level and low frequency spread, delineated by spot-density contours, indicative of one-hop propagation.
2. An arc of spots (orange) with lower signal level and over 100mHz frequency spread indicating two-hop side scatter [4], [5]. This propagation mode prevails when the operating frequency is above the maximum useable frequency (MUF). Given the north-south geometry of W7WKR to KPH, and the local time of day, morning, the side scatter probably took place near the intersection of 1100km arcs from the stations to the east.
3. An arc of spots (green) with high signal level and high frequency spread. This combination suggests those spots were decoded when ray landing spots were within a narrow zone with two-ray arrivals at the receiver. What constitutes the two-ray zone is described next.

Two-ray zone

Low-elevation rays are associated with long-range propagation: as elevation increases, the range reduces. This is well known. However, if the operating frequency is above foF2, there will be a fold-back in range at some point. This means there exists a zone, starting at the ray landing spot closest to the transmitter, where a receiver would receive signals via two ordinary rays [12] (see **Figure 6**). At 14MHz on eclipse day, the two-ray zone on this path occurred over 5° of elevation from 24° to 29°. The ray at 26.7° gave shortest range, the dashed line at 1010km. This delineates the end of the skip zone that started at the ground-wave limit. The second dashed line marks the end of the two-ray zone; rays at higher angles passed through the ionosphere.

The frequency spread observations on the W7WKR to KPH path, and

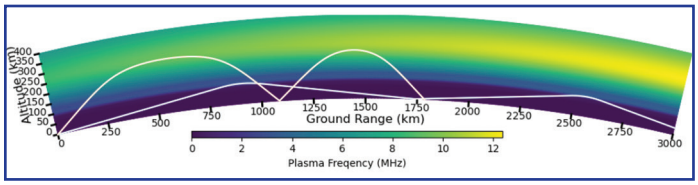

FIGURE 4: Ray traces from PyLap, showing two-hop and one-hop propagation with SSNe of 125 for 14 October 2023 at 1630UTC on 14.097MHz on the path between W7WKR and KV6X.

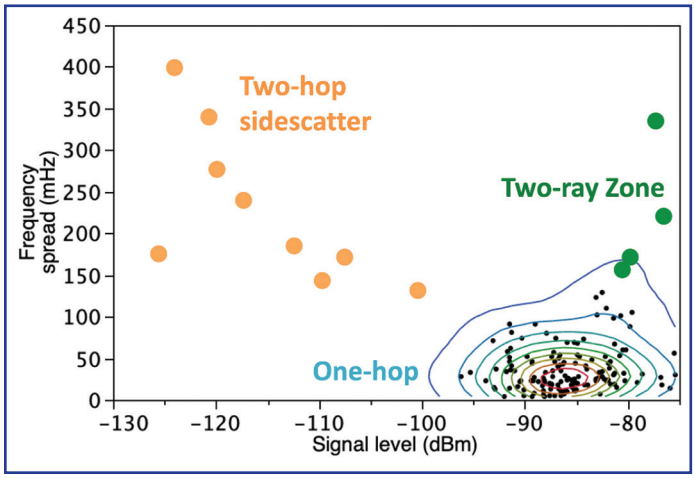

FIGURE 5: Scatter plot of frequency spread against signal level for the 14MHz FST4W transmissions from W7WKR, received at KPH over a path of 1056km, on 14 October between 1442UTC and 2000UTC.

Gwyn Griffiths, G3ZIL
gxgriffiths@virginmedia.com

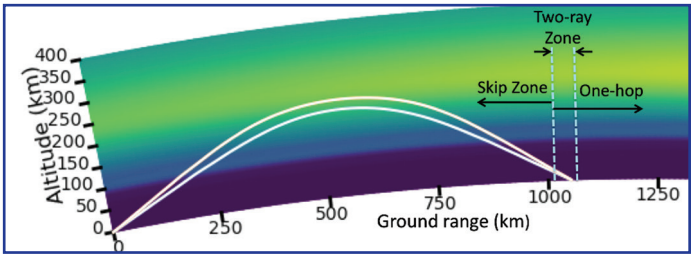

FIGURE 6: PyLap ray trace showing the paths of two ordinary rays launched at W7WKR at 24° and 29°; both land at the same point within the two-ray zone.

the three propagation modes, are brought together in **Figure 7**. Figure 7(a) is a time series of frequency spread around the eclipse maximum. There's an arrow from one example of each propagation mode to a ray elevation against range graph on the right. All one-hop spots (low frequency spread) are in the region with one ray arrival path, Figure 7(b). Spots with high signal level and high frequency spread (green) would be from the two-ray zone, with two ray paths to the receiver, Figure 7(c). Intuitively, two ray paths to a receiver could explain higher signal levels, albeit with multi-path fading, and higher frequency spread from refraction at different heights. The two-ray zone would shift across KPH as the MUF dropped and the propagation zone moved out in range. When the MUF dropped further, placing KPH within the skip zone, propagation would be via two-hop side scatter, Figure 7(d).

What did not happen as the eclipse progressed was a simple single transition from one-hop to two-ray zone to two-hop backscatter and back again. Rather, the observations suggest a more-complex picture. The first event was indeed the ideal transition sequence, between 1610UTC and 1630UTC. Next was an interval with an MUF high enough to support one-hop until 1640UTC. The MUF then dropped low enough, and sufficiently fast, for no observation within the narrow two-ray zone. This was soon followed by a fast recovery, and another fast drop at 1654UTC. The subsequent recovery was slow enough to give one spot in the two-ray zone at 1704UTC. A final drop in MUF at 1712UTC was shallow; it only shifted propagation to the two-ray zone, after which no further effects from the eclipse were seen.

At KFS, 70km further south of KPH on a 189° heading rather than 193° from W7WKR, there were no transitions to two-hop side scatter; however, there were twelve instances of spots in the two-ray zone. This suggests that the skip zone, Figure 7(d), did not migrate further than 1126km from W7WKR.

End note

The implication of these observations is that there were short-period changes of ionisation and/or height in the F2 refracting layer modulating the slow eclipse obscuration function. Those short-period changes resulted in at least four cycles of to-and-fro motion of the ray-landing spots as identified in Figure 6. In a subsequent article, I'll show how Doppler shift measurements from FST4W were used to calculate the height of refraction and its variation during the eclipse. All of these data are in the public domain, together with access tools [6].

Table 1: Mean frequency spread (in mHz) in 20-minute intervals centred on the times listed for the eclipse day, and four unaffected days, on the 1808km path W7WKR and KV6X on 14.097MHz. After the maximum obscuration at 16:37UTC, the low values suggest one-hop propagation only.

	11th Oct	12th Oct	13th Oct	14th Oct	15th Oct
16:20	103	146	503	198	265
16:40	163	147	144	89	145
17:00	126	74	316	8	120
17:20	131	168	238	21	130
17:40	148	147	137	197	140
18:00	172	155	348	101	190
18:20	168	153	193	88	127

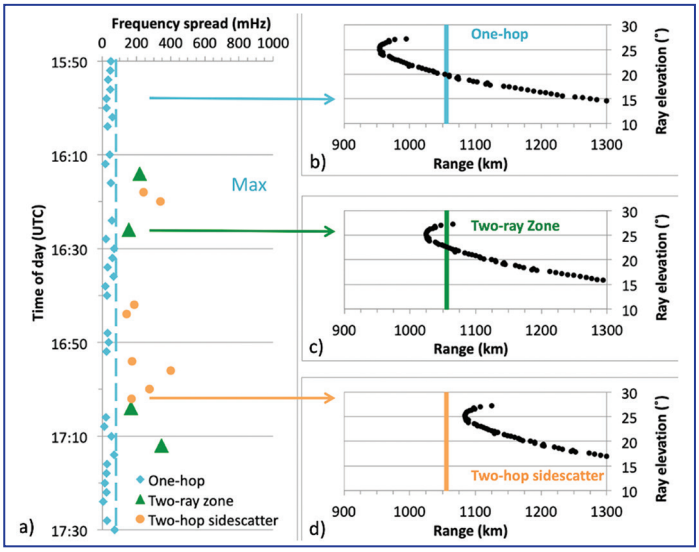

FIGURE 7: Three propagation modes during the eclipse on the 1056km path between W7WKR and KPH at 14MHz (eclipse start at 1506UTC, and end at 1742UTC). KPH range from W7WKR is the vertical line. (a) Time series of frequency spread showing spots via one-hop (cyan), from the two-ray zone (green), and via two-hop side scatter (orange). (b) Range of the landing spots for rays leaving W7WKR when the MUF sustained plain one-hop to KPH. (c) MUF has reduced: KPH is within the two-ray zone. (d) MUF has reduced further: there is no direct path to KPH, but none of the spots at KFS, 70km further south, were within this zone.

Acknowledgments

I am grateful to Rob Robinett, AI6VN for WsprDaemon, and the WSJT-X development team for FST4W. PyLap uses the HF propagation toolbox, PHaRLAP, created by Dr. Manuel Cervera, Defence Science and Technology Group, Australia, available by request from [13]. Specific data for this article came from Tom Bunch, WO7I; Paul Elliott, WB6CXC; Dick Bingham, W7WKR; Dan Beugelmans, KV6X and the late Craig McCartney, W6DRZ; KFS Radio Club and Globe Wireless Radio Services for KFS; and the Maritime Radio Historical Society for KPH.

References

[1] https://hamsci.org/eclipse
[2] G. Griffiths et al., 2022. FST4W on the HF bands: Why - What to expect - Equipment - Results, Proc. ARRL/TAPR Digital Communications Conference 2022, pp. 12–22, available at https://files.tapr.org/meetings/DCC_2022/2022%20DCC1.pdf
[3] G. Griffiths et al., 2020. Estimating LF-HF band noise while acquiring WSPR spots. ARRL QEX, September-October 2020.
[4] G. Griffiths. Insights into HF propagation using FST4W. RadCom, 99(9), 30-32.
[5. G. Griffiths. Identifying 14 MHz propagation modes using FST4W SNR and spectral spread. ARRL QEX, May-June 2024.
[6] http:/wsprdaemon.org
[7] S. Nichols. Partial eclipse 2015: Solar eclipse propagation experiments yield valuable data. RadCom, 91(6): 22-26.
[8] The WsprSonde, designed and developed as a propagation research tool by Paul Elliott, WB6CXC, is capable on simultaneous transmissions on six or eight HF bands: https://turnislandsystems.com/
[9] A. M. Price-Whelan et al., 2018. The Astropy project: building an open-science project and status of the v2. 0 core package. The Astronomical Journal, 156(3), p.123. Available via https://www.astropy.org/
[10] Radio Communication Handbook, 2020. M. Browne (editor), RSGB. Page 12.14.
[11] https://github.com/hamsci/pylap
[12] Two extraordinary rays will also arrive at the receiver via slightly different azimuth and elevation paths from the ordinary rays. However, their presence is an additional detail, not essential to this introductory description.
[13] manuel.cervera@dsto.defence.gov.au